

Article

# Natural and Anthropogenic Factors Shaping the Shoreline of Klaipėda, Lithuania

Vitalijus Kondrat \*, Ilona Šakurova, Eglė Baltranaite  and Loreta Kelpšaitė-Rimkienė 

Marine Research Institute, Klaipėda University, Universiteto Ave. 17, LT-92294 Klaipėda, Lithuania; ilona.sakurova@ku.lt (I.Š.); egle.baltranaite@ku.lt (E.B.); loreta.kelpsaite-rimkiene@ku.lt (L.K.-R.)

\* Correspondence: vitalijus.kondrat@ku.lt

**Abstract:** Port of Klaipėda is situated in a complex hydrological system, between the Curonian Lagoon and the Baltic Sea, at the Klaipėda strait in the South-Eastern part of the Baltic Sea. It has almost 300 m of jetties separating the Curonian Spit and the mainland coast, interrupting the main path of sediment transport through the South-Eastern coast of the Baltic Sea. Due to the Port of Klaipėda reconstruction in 2002 and the beach nourishment project, which was started in 2014, the shoreline position change tendency was observed. Shoreline position measurements of various periods can be used to derive quantitative estimates of coastal process directions and intensities. These data can be used to further our understanding of the scale and timing of shoreline changes in a geological and socio-economic context. This study analyzes long- and short-term shoreline position changes before and after the Port of Klaipėda reconstruction in 2002. Positions of historical shorelines from various sources were used, and the rates (EPR, NSM, and SCE) of shoreline changes have been assessed using the Digital Shoreline Analysis System (DSAS). An extension of ArcGIS K-means clustering was applied for shoreline classification into different coastal dynamic stretches. Coastal development has changed in the long-term (1984–2019) perspective: the eroded coast length increased from 1.5 to 4.2 km in the last decades. Coastal accumulation processes have been restored by the Port of Klaipėda executing the coastal zone nourishment project in 2014.

**Keywords:** Baltic Sea; Port of Klaipėda; shoreline changes; DSAS; clusterization; regime shift detection; dredging; sand nourishment



**Citation:** Kondrat, V.; Šakurova, I.; Baltranaite, E.; Kelpšaitė-Rimkienė, L. Natural and Anthropogenic Factors Shaping the Shoreline of Klaipėda, Lithuania. *J. Mar. Sci. Eng.* **2021**, *9*, 1456. <https://doi.org/10.3390/jmse9121456>

Academic Editor: Carlos Daniel Borges Coelho

Received: 18 November 2021  
Accepted: 17 December 2021  
Published: 20 December 2021

**Publisher's Note:** MDPI stays neutral with regard to jurisdictional claims in published maps and institutional affiliations.



**Copyright:** © 2021 by the authors. Licensee MDPI, Basel, Switzerland. This article is an open access article distributed under the terms and conditions of the Creative Commons Attribution (CC BY) license (<https://creativecommons.org/licenses/by/4.0/>).

## 1. Introduction

Erosion is a significant problem affecting sandy beaches that will worsen with climate change and anthropogenic pressure. Sandy shorelines are highly dynamic due to altering wave conditions, sea levels and winds, geological factors, and human activity [1]. Therefore, identifying the most vulnerable areas to erosion is crucial for nearshore communities since it could significantly affect their socio-economic state through destruction of infrastructure, loss of land and property on the coast, and valuable beach areas used for recreation.

Shore regeneration is a slow process lasting for more than one year, while erosion usually occurs in a matter of a few days, making it difficult to detect visually. As short-term measurements do not reflect actual multi-annual dynamic trends, studies involving several shoreline decay and regeneration cycles are necessary to determine long-lasting changes in the shoreline dynamics. Typically, coastal research to assess and predict long-term shoreline dynamics and the erosion rates is based on the data covering up to 10 years (short-term), 10–60 years (medium-term), and more than 60 years (long-term) of shoreline position [2–4].

Shoreline dynamics depend on different causes, mainly on the sediments in the sea-land system [5–7]. Furthermore, the different coastal stretches have particular favorable hydrometeorological conditions for the accumulation or erosion processes. The rapid urbanization of the coastal zone has a significant impact on shoreline development [8–10]. Sustainable coastal development requires knowledge of the coastal processes

combined with incorruptible urbanization and properly chosen shoreline erosion mitigation methods [10,11]. Often, an insufficient understanding of the coastal processes causes costly incidents.

A number of studies [8,12,13] show the impact of anthropogenic factors in particular port activities on shoreline positions. Erosion and accumulation are naturally occurring processes that often coincide in a dynamic equilibrium [14]. However, increasing anthropogenic pressure at the coast has disrupted the natural development of the coast, accelerating erosion processes in some places and causing accumulation in others [14]. Analysis of shoreline changes is a well-developed field that has progressed complex data processing and analytical protocols [15]. However, quantifying coastal development trends is only one aspect of the problem; it is necessary to understand the drivers of change and address local impacts in a broader regional context that is important from a decadal to a centennial timescale [15]. Understanding the causes of atypical coastal development is important to make sustainable coastal zone management plans. Such knowledge is crucial not only for the coastal dynamics experts, but also for the port managers, as it can serve as the basis for future decisions on how to reduce port damage to the coasts.

This paper analyses the shoreline dynamic in the context of climate change and increased anthropogenic pressure, focusing on identifying long- and short-term shoreline movement tendencies and identifying the direct impact zone of the Port of Klaipėda. As well as answering the question of whether and how shoreline evolution is affected by the artificial sand nourishment carried out in accordance with the Port of Klaipėda management plan.

## 2. Study Site

The Lithuanian coast of the Baltic Sea represents a generic type of almost straight, relatively high-energy, actively developing coasts that (i) contain a large amount of fine mobile sediment; (ii) are open to predominating wind and wave directions; and (iii) are exposed to waves from many directions [16]. The study area extends 10 km from Klaipėda seaport jetties to the north and 10 km to the south. This particular area was chosen based on the following aspects: (i) the broad demand spectrum of recreational uses [17]; (ii) the high risk of coastal erosion [18,19]; (iii) the possibility of direct and indirect anthropogenic impacts [20,21].

The South-Eastern coast of the Baltic Sea is formed by the presence of the Port of Klaipėda [21,22]. Historically, the Port of Klaipėda has been known from the 13th century when vessels of Lubeck and Bremen merchants used to moor in the small port neighboring the Klaipėda castle [23]. Port expansion to the Klaipėda strait started in 1745, and the chronicle of 1797 mentions that Port of Klaipėda consists of the Dane river port and a big water basin in the strait of the Curonian Lagoon. In the 19th century, wooden jetties were constructed [22]. 1924–1939 was a period when Klaipėda seaport was at its flourishing peak—new stony jetties and quays were assembled [24,25]. Since the occurrence of the first jetties, ongoing coastal engineering problems were encountered relating to wave exposure, siltation within the port, extensive dredging requirements, and seiching within the confines of the present harbor [22,26].

After the construction of the first port jetties, at the end of the 19th century, the shoreline moved seawards significantly on both sides of the jetties [20]. This insight raises doubts about the predominant sedimentary direction from south to north [6]. The dumping of the dredged sand can partly explain this accumulation tendency in the northern part of the jetties from the Klaipėda strait [22]. Up until the beginning of the 20th century, sand dredged from the port had been dumped at shallow depths north of the jetties, initiating coast accumulation [22].

After the prolongation and construction of new concrete jetties at the beginning of the 20th century (works finished till 1934) [21] alongside changed dredging policies [13], observations were made that sand dredged next to the port jetties returns into the inlet and continues dredging works to ensure the depth of the entrance channel.

Due to depth restrictions in the Danish Straits, vessels with a maximum draft of 16.5 m, and in some cases, vessels with a draft of up to 17 m can enter the Baltic Sea. Another limitation for ships entering the Baltic Sea is the bridge height to about 65 m entering the strait of the Great Belt, which connects the Danish islands of Zealand and Funen. These restrictions prevent vessels with a draft greater than 16.5 m from entering the Baltic Sea from those of Class Panamax (Baltmax). The long-term competitiveness and sustainability of the Klaipėda seaport can be ensured only by increasing the technical capability of the port to receive and service ships of the maximum capacity [27].

Therefore, in 1999, the final design for reconstruction of the Port of Klaipėda jetties was established. The seaport jetties system was reconstructed by narrowing the entrance channel and changing the position of the northern pier. In 2002 the northern pier was extended by 205 m (up to 733 m) and the southern pier by 278 m (up to 1374 m) (Figure 1) [28]. At the same time, the entrance channel was dredged to a depth of 14.5 m. According to the recent port development plan, the entrance channel will be dredged up to 17 m by 2023.

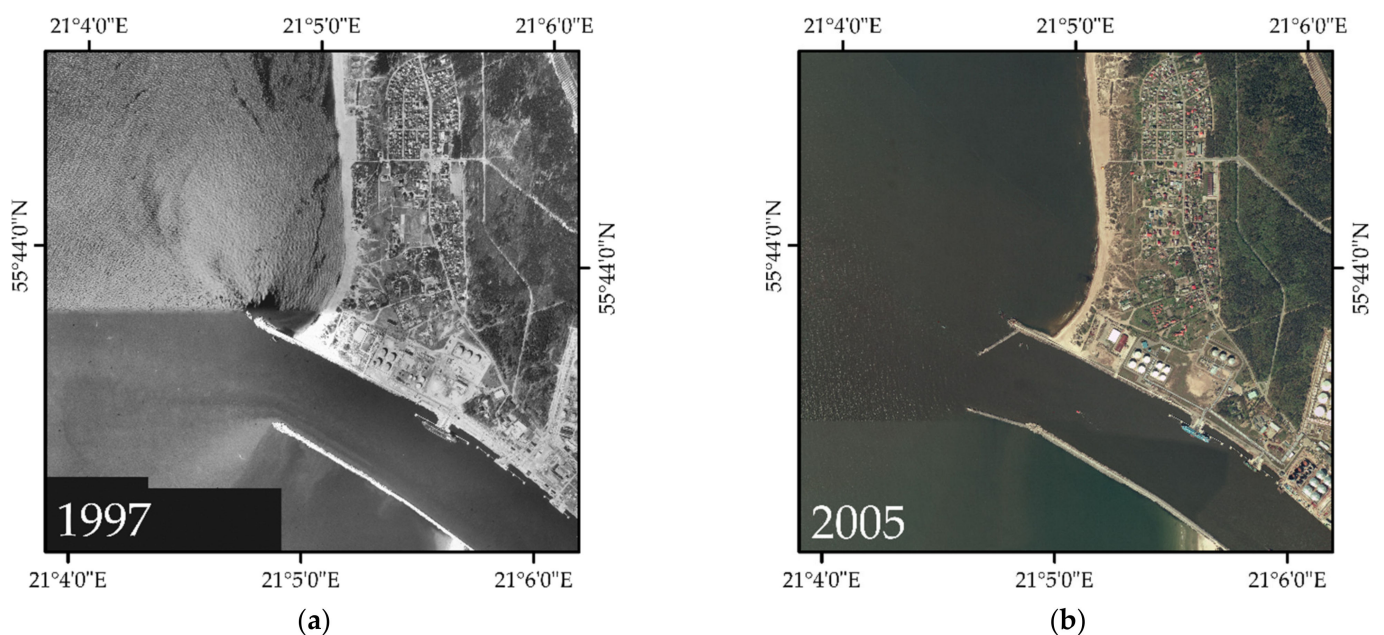


**Figure 1.** The Klaipėda seaport jetties before and after the reconstruction of 2002, (a) 1997, and (b) 2005.

The Port of Klaipėda, located at the Klaipėda strait (Figure 2) (South-Eastern coast of the Baltic Sea), divides the Lithuanian coast into two geologically and geomorphologically different parts: southern—the coast of the Curonian spit, northern—mainland coast (Figure 3) [29]. Port jetties interrupt the main sediment transport path and significantly influence the Lithuanian coast's northern (38.49 km long) part [6,20]. Only Quaternary sediments are found on the Lithuanian coast of the Baltic Sea [6,30]. From the geological point of view, the mainland coast and the Curonian Spit coast are not homogenous (Figure 4). The geological structure of the mainland coast was mainly determined by the sediments formed during the last few glaciations. The sediments of the Curonian Spit coast were formed in the Baltic Sea basin—starting with the Baltic Ice Lake and ending with the modern Baltic Sea [6,30].

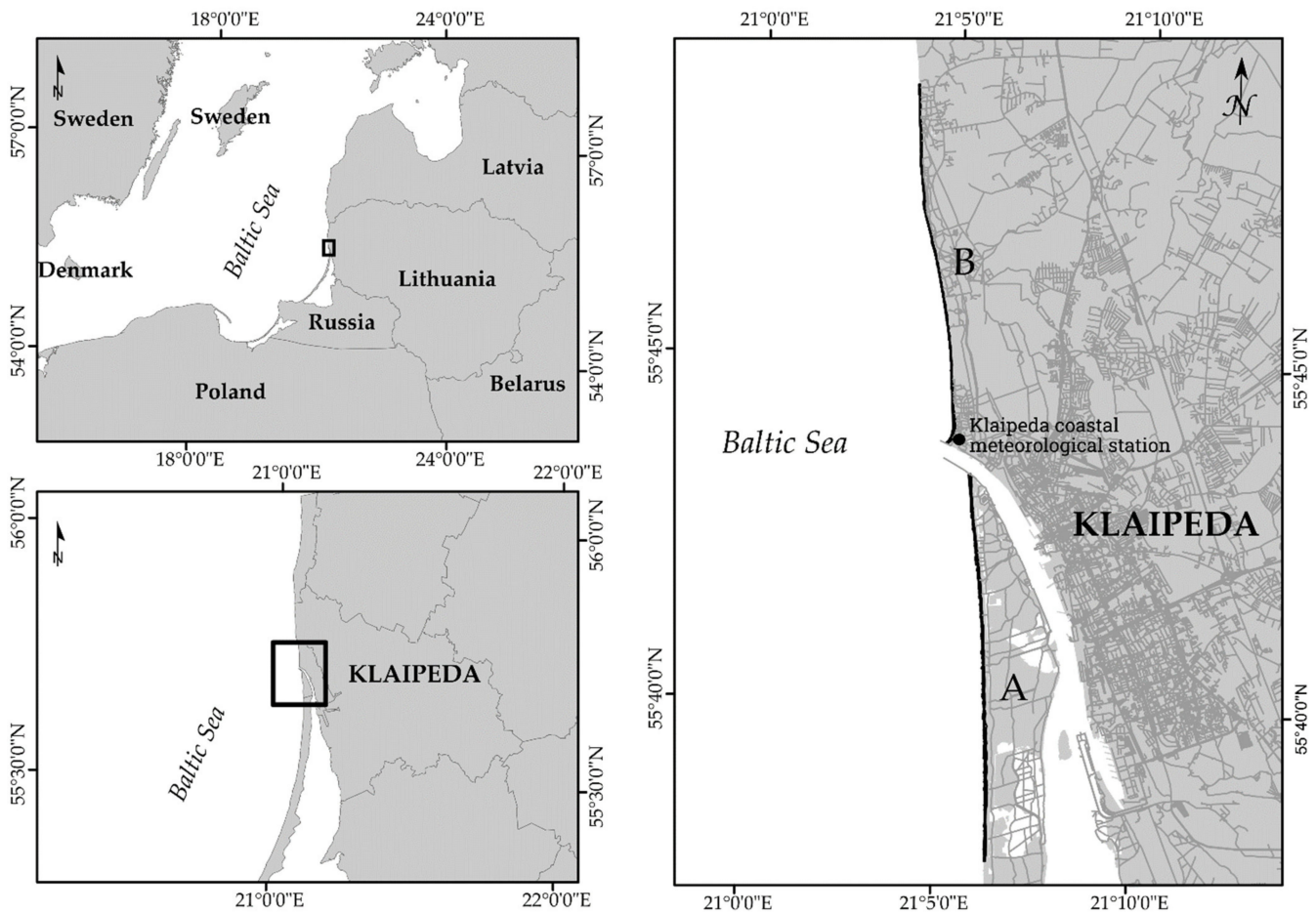


**Figure 2.** Location of the study site in the south-eastern Baltic Sea, A: the Curonian Spit coast, B: the mainland coast.

The sandy sediments form the part of the Curonian Spit coast: this Lithuanian coastal sector is characterized by accumulation relief [6]. The mainland coast of Lithuania is geologically heterogeneous: the northern part of the mainland coast is mainly formed of fine-grained sand (0.25–0.1 mm), while the southern and central parts of the mainland coast are formed by the medium-grained (0.5–0.25 mm) and coarse-grained (1–2.5 mm) sand [6,14]. A detailed description of the Lithuanian coast geomorphological and geological structure is provided by Bitinas et al. (2005)

According to the granulometric analysis of sediment samples from 2019 along the study area (Figure 4), on the Curonian Spit coast (A, a), very well and moderately sorted ( $\sigma = 1.21\text{--}1.47$  mm) fine sand ( $Md = 0.20\text{--}0.37$  mm) prevails, while on the mainland coast (B, b, c), the sorting of the sediments differs in a cross-shore profile. In profile *b*, moderately well-sorted ( $\sigma = 1.44$  mm) medium sand ( $Md = 0.32$  mm) prevails in a shoreline area, well-sorted ( $\sigma = 1.19$  mm) slightly very fine gravelly medium sand ( $Md = 0.21$  mm) prevails in a beach area, and moderately well-sorted ( $\sigma = 1.47$  mm) sand prevails ( $Md = 0.36$  mm) in a foredune area. In profile *c*, poorly sorted ( $\sigma = 3.84$  mm) very fine gravelly fine sand ( $Md = 0.24$  mm) prevails in a shoreline area, poorly sorted ( $\sigma = 10.69$  mm) medium gravelly fine sand ( $Md = 0.23$  mm) prevails in a beach area, and poorly sorted ( $\sigma = 18.21$  mm) sandy very fine gravel prevails ( $Md = 1.12$  mm) in a foredune area.



**Figure 3.** Study site shoreline features: (a) the Curonian Spit coast Smiltynė I beach (© I. Šakurova); (b) the Curonian Spit coast Smiltynė I beach (© I. Šakurova); (c) the mainland coast Giruliai beach (© L. Kelpšaitė-Rimkienė); (d) the mainland coast Melnragė I beach (© V. Kondrat).

During the dredging of the Klaipėda strait, the glaciogenic moraine deposits and alluvial sediments are mainly excavated—sand (0.002 mm 10–30%–2 mm 50%) and silt (0.002 mm 10–30%–2 mm 30–50%). All lithological sediment types are dumped in dumping area I (Figure 4) at a depth of 45–50 m. The II dumping area (Figure 4) is intended only for the dumping of sandy sediments—fine (0.25–0.1 mm > 50%) and aleuritic (<0.063 mm 10–30%) sand at a depth of 28–35 m. Since 2001, clean sand that meets sanitary–hygienic requirements excavated from the port entrance channel has been dumped in the dumping area III (Melnragė–Giruliai) at a 4–6 m depth. This area is intended to replenish the sediment balance and restore beach sand reserves [24].

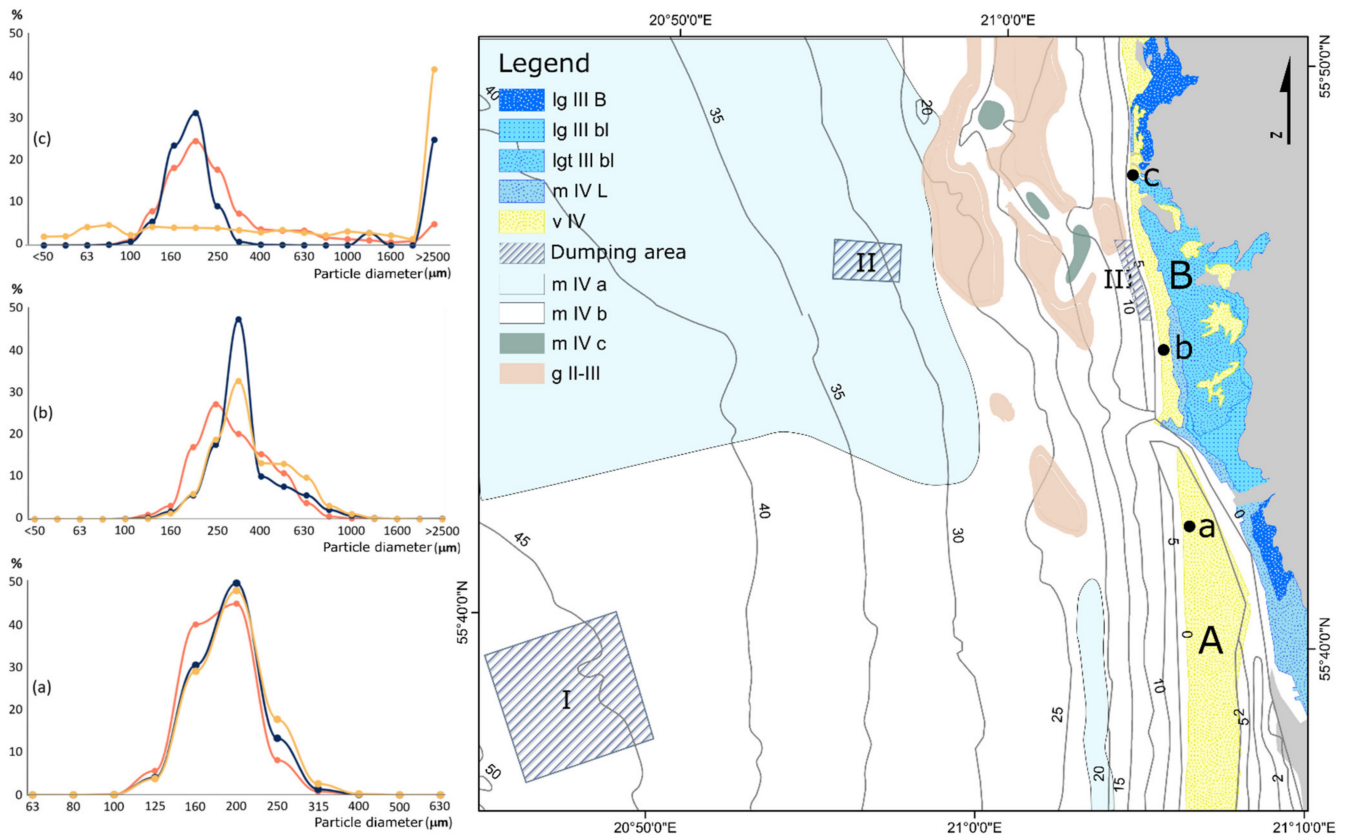


**Figure 4.** Map of Quarternary sediment type of coastal area and dumping zones of dredging material. Lg III B—glaciolacustrine sediments of the Baltic Ice Lake (fine sand); lg III bl—glaciolacustrine sediments (various sand); lgt III bl—marginal glaciolacustrine deposits (fine sand); m IV L—Litorina Sea sediments (fine sand); v IV—aeolian deposits (fine sand); m IV a—nearshore sediments (extra fine sand (0.05—0.1 mm)); m IV b—nearshore sediments (fine sand (0.1—0.25 mm)); m IV c—nearshore sediments (gravel with sand); gII-III—glacial deposits of Middle and Upper Pleistocene (unseparated), glacial loam, boulders and gravel (washed till). I—distant dumping area; II—near dumping area; III—nearshore dumping area (adapted from Bitinas et al., 2004). Grain-size composition of surface sediments at Smiltynė I (a), Melnragė I (b), and Karklė (c). Orange color line—western part of the dunes (foredune); blue line—the middle of the beach; red line—a dynamic shoreline in July of 2019.

### 3. Materials and Methods

#### 3.1. Analysis of Cartographical Data

In this paper, we evaluate a period of 35 years of shoreline position variation tendencies for 1984–2019. All shoreline position changes were determined using the available high accuracy (1:10,000) cartographic data for the years: 1984, 1990, 1995, and 2005 (Table 1) obtained from Lithuania’s National Land Service under the Ministry of Agriculture and GPS survey data for 2015 and 2019. The shoreline position was established at the middle of the swash zone by dual-band GPS receiver “Leica 900”.

Shoreline position changes were analyzed with the ArcGIS extension DSAS v. 5.0 (Digital Shoreline Analysis System) package, developed by the United States Geological Survey (USGS) [31,32]. The DSAS is executed in five steps: (1) shorelines digitizing and uniforming to WGS-84 coordinate systems (UTM Zone 34); (2) computation of the uncertainties; (3) baseline creation and transects generation; (4) computation of distances between baseline and shorelines at each transect; and (5) computation of shoreline change statistics.

Three statistical parameters—net shoreline movement (NSM), end-point rate (EPR), and the shoreline change envelope (SCE)—were estimated and analyzed along with each transect every 25 m along the shoreline (796 transects in total). NSM values report the net change of the shoreline in the study period between the oldest and most recent shoreline.

EPR rate (m/yr) indicates change rates between the earliest and most recent shoreline positions. SCE capacity provides the envelope of shoreline variability, and it is the only measure of the total shoreline change among all the available shoreline positions [33].

**Table 1.** Shoreline positioning and detection errors. Ed—digitization error, Ep—pixel error, Es—sea-level fluctuation error, Ec—shoreline line detection or resolution errors, Etc—T-sheets plotting errors, Er—rectification error, Ut—shoreline capture error.

Data Source	Errors (m)						
	Ed	Ep	Es	Ec	Etc	Er	Ut
T-Sheets (1984)	2.961	0.987	0.680	3.948	7.500		9.058
T-Sheets (1990)	2.760	0.920	0.570	2.680	7.500		8.498
Orthophotos (1995)	2.500	0.506	0.490	2.024		0.500	3.331
Orthophotos (2005)	2.500	0.513	0.720	2.052		0.500	3.390
GPS (2010)			0.590	0.295			0.660
GPS (2015)			0.610	0.295			0.678
GPS (2019)			0.570	0.295			0.642

### 3.2. Data Reliability and Limits of Uncertainty

The shoreline position is highly variable in short time scales due to heavy storms, waves, and wind setup when extreme natural variations induce significant temporary shoreline retreat. Mapping the historical shorelines introduces additional uncertainties [34]. Although most researchers have similar techniques for estimating shoreline value changes, the methodology used to estimate changes varies considerably, significantly altering the accuracy and reliability of the data collected or determined. The dynamics of the shore itself may also cause certain differences and inaccuracies in shoreline surveys. Therefore, the values of the same shoreline determined by two independent scientists in the same field of science can vary considerably in their size and accuracy [35].

The most significant differences in the data occur during the digitization and processing of cartographic material. The differences in the values of shoreline changes may also occur due to the different statistical research methods used to determine the degree of shoreline change (shoreline change rate). The primary data and the analysis methods are the main factors defining the shoreline variations and accuracies. Therefore, prior to choosing a statistical research method, it is imperative to estimate the errors in determining the shoreline position in the cartographic material [36].

In this study, we determined three shoreline positioning and detection errors (Table 1) based on [14,36,37]:

The error in the position of the shoreline when determining in the T-Sheets:

$$Ut = \pm (Ed^2 + Ep^2 + Etc^2 + Es^2 + Ec^2)^{1/2} \tag{1}$$

The positioning error of the shoreline in orthophotos equals:

$$Ut = \pm (Er^2 + Ed^2 + Ep^2 + Es^2 + Ec^2)^{1/2} \tag{2}$$

GPS data error:

$$Ut = \pm (Es^2 + Ec^2)^{1/2} \tag{3}$$

Here: Ut—shoreline capture error, Er—rectification error, Ed—digitization error, Ep—pixel error, Ets—photo plan creation error, Ec—shoreline line detection or resolution errors, Eg—georeferencing error; Es—sea-level fluctuation error; Etc—T-sheets plotting errors.

The shoreline uncertainty limit for different periods is equal to the sum of the shoreline fixation errors for different periods:

$$\sum Ut = (Utn_1 + Utn_2 + Utn)^{1/2} \tag{4}$$

Here  $n_1, n_2,$ —shoreline detection errors for different periods.

The shoreline uncertainty threshold (minimum time criterion) in the statistical methods for determining shore change (EPR) equals:

$$\sum Ut/n \tag{5}$$

Here  $n$ —research period.

### 3.3. Clusterization

K-Mean cluster analysis for the net shoreline movement (NSM) values was applied to identify shoreline zones with similar evolution tendencies [38]. The K-means algorithm is a simple and popular clustering approach used in various applications [39]. It is a point-based clustering approach that starts with cluster centers located initially in arbitrary locations and goes through each stage of the cluster center to reduce the cluster error [39–41].

$$E = \sum \|X_i - m_i\|^2 \tag{6}$$

where  $E$  is the sum of squared errors for all objects in the data,  $X_i$  is the point in a cluster, and  $m_i$  is the mean of cluster  $k_i$ . The objective of K-means is to minimize the sum of squared errors over all  $k$  clusters. The algorithm first places  $k$  points in the space represented by the objects clustered as initial group centroids. The second step is to assign each object to the nearest cluster center. Then, the mean of each cluster is calculated to obtain a new centroid. These steps are repeated until the centroids do not change. The within-cluster sum of squares measures the variability of the observations within each cluster. In general, a cluster with a small sum of squares is more compact than a cluster with a large sum of squares [38,39]. Clusters with higher values exhibit more significant variability of the observations within the cluster [38,39]. The number of clusters is chosen based on the elbow method [38], whose main idea is to define groups such that the total intra-cluster variation (or the total sum of squares within clusters (WSS)) is minimized. In this case, the elbow of the curve is formed for the five clusters (Figure 5).

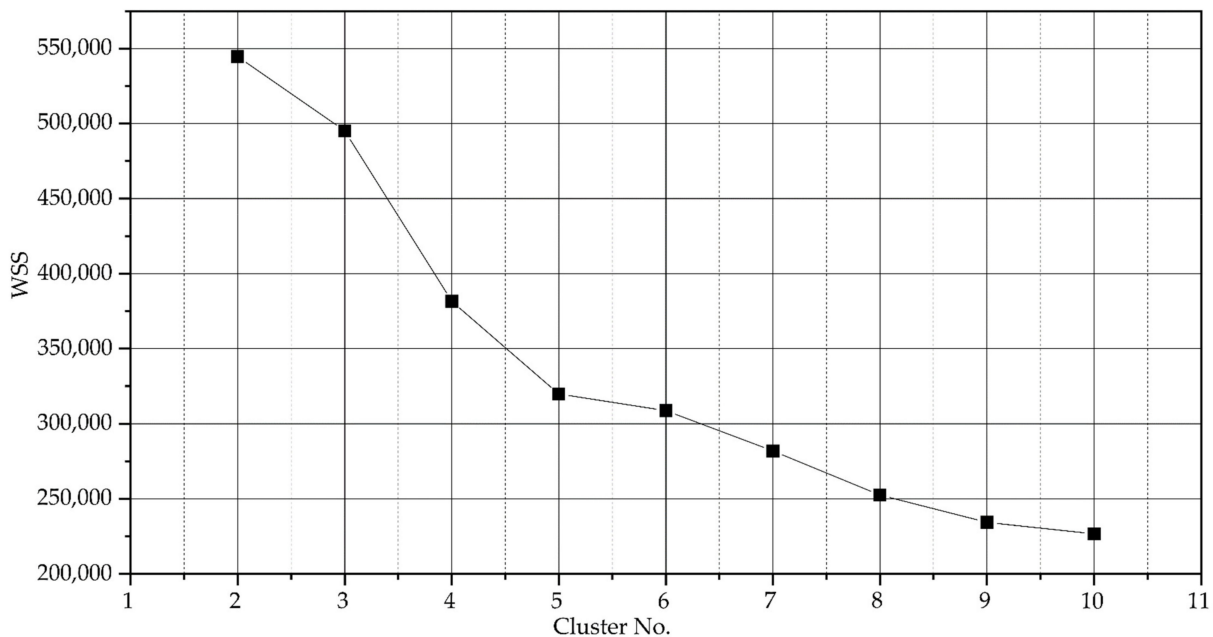


Figure 5. The number of clusters is chosen based on the within-cluster sum of squares parameter.



### 3.4. Analysis of Meteorological Data

The meteorological data (annual mean wind speed and direction) of the 1960–2019 time period were analyzed to detect the wind direction’s regime shift. The meteorological data were acquired from the Marine Environment Assessment Division of the Environmental Protection Agency (EPA) and derived from the Klaipėda coastal meteorological station (Figure 2) under the Lithuanian Ministry of Environment’s environmental monitoring program. The program has been prepared in line with the legislation of the European Union.

A STAR (Sequential T-test Analysis of Regime Shifts) algorithm was applied to determine regime shifts in the analyzed time series (<https://www.beringclimate.noaa.gov/> (accessed on 10 October 2021)). The algorithm was built upon a sequential *t*-test that can signal the possibility of a real-time regime shift [42]. The algorithm can process the data regardless of whether it is presented in anomalies and/or absolute values or not. It can automatically calculate regime shifts in large sets of variables [42].

For this study, the following set of input parameters were used: cut-off length (I) was set to 10 years; Hubert’s weight parameter (HWP) was set to 1. HWP determined the weight of outliers in the calculation of average values of the regime shift. The confidence level was set to 0.1.

## 4. Results

### 4.1. Long-Term Shoreline Changes

NSM for the entire study period 1984–2019 showed (Figure 6) that 60.43% of the shoreline was accumulative, 20.98% erosive, and 18.59% was stable or within the range of uncertainty  $\pm 9.08$  m (Table 2). Generally, the studied coast can be described as accumulative with the average  $14.46 \pm 1.92$  m shoreline movement offshore tendency; the average shoreline movement velocity was  $0.42 \pm 0.03$  m/year.

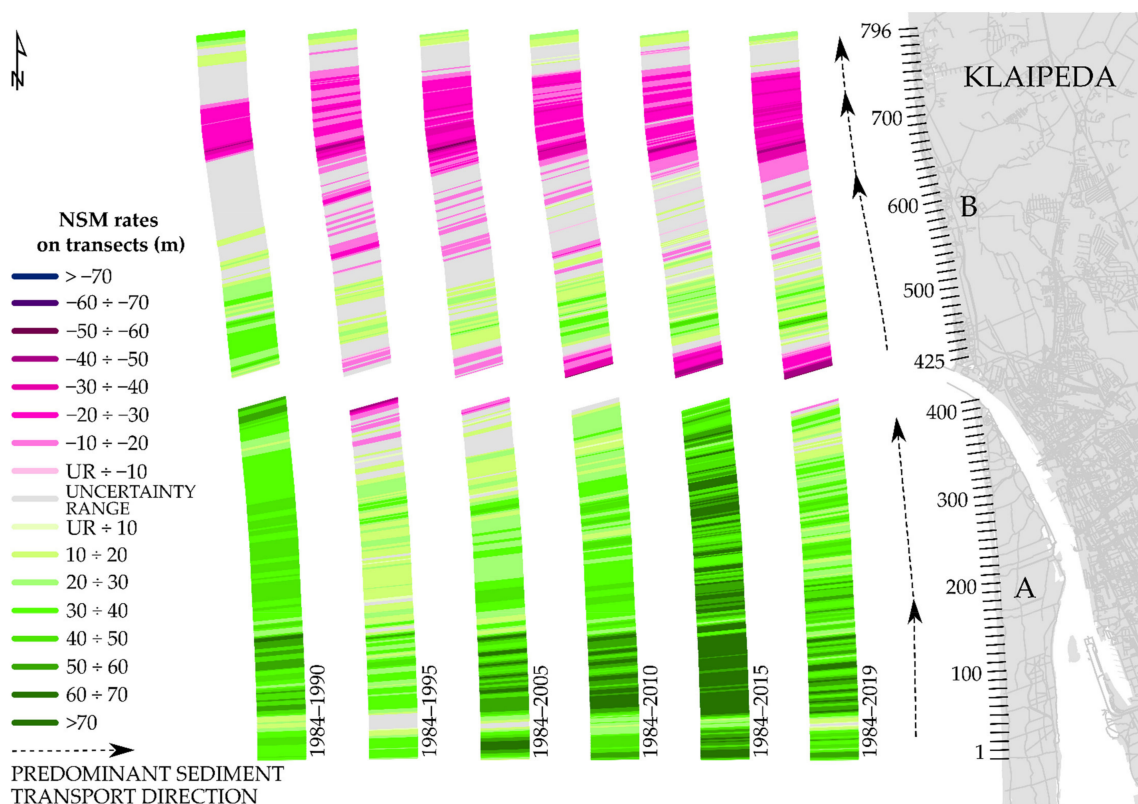


**Figure 6.** Net Shoreline Movement (NSM) rates 1984–2019 short-term vs long-term tendencies on the Curonian Spit coast (A) and the mainland coast (B). Annual shoreline change rates are shown on the transects graph. Purplish color tones on the transects indicate a trend of coastal erosion, while green tones indicate a trend of accretion, and grey color indicates shoreline variation values in its positioning and detection uncertainty range. Numbers and lines on the A and B coasts indicate transects distribution along the study site.

Table 2. Shoreline uncertainty range.

Years	±Uncertainty Range		Years	±Uncertainty Range	
	(m)	(m/yr)		(m)	(m/yr)
1984 * and 1990 *	±12.42	±2.07	1990 * and 1995 **	±9.13	±1.83
1984 * and 1995 **	±9.65	±0.88	1995 ** and 2005 **	±4.75	±0.48
1984 * and 2005 **	±9.67	±0.46	2005 ** and 2010 ***	±3.45	±0.69
1984 * and 2010 ***	±9.08	±0.35	2010 *** and 2015 ***	±0.95	±0.19
1984 * and 2015 ***	±9.08	±0.29	2015 *** and 2019 ***	±0.93	±0.23
1984 * and 2019 ***	±9.08	±0.26			

\* T-Sheets; \*\* Orthophotos; \*\*\* GPS.

Comparing trends of shoreline changes in 1984–2019, we found that the accumulation processes on the shores of the Curonian Spit accounted for 96.12% (396 out of 412) of transects. The shoreline moved towards the sea at an average speed of  $1.01 \pm 0.02$  m/year (Figure 7), with the highest rates of the EPR 2.15 m/year. The NSM value was  $35.97 \pm 0.69$  m, stable shoreline changes were found in 3.64% of transects and erosions in 0.24% of transects. The highest intensity of erosion processes at the Curonian Spit was recorded in 1984–1995. The negative shoreline shift towards the mainland was found in 6.07% (25 out of 412) of transects, where the average NSM value was  $-19.38 \pm 2.50$  m. Stable shoreline changes were found in 18.69% (77 of 412) of transects, and accumulation was detected in 75.24% (310 of 412) of transects with an accumulation rate of  $2.17 \pm 0.05$  m/year, NSM value was  $23.86 \pm 0.52$  m.

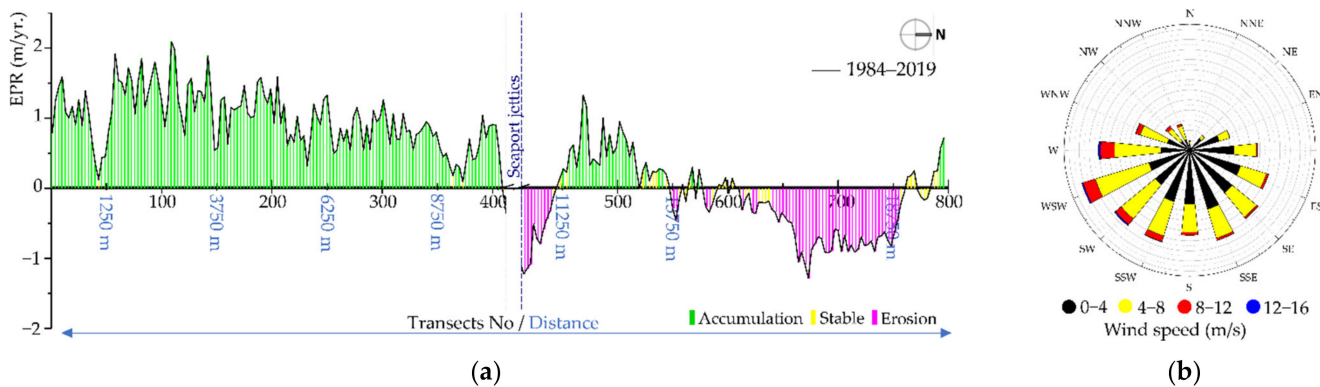


Figure 7. Graph showing the distribution of EPR (a) and wind rose (b) for 1984–2019.

In 1984–2019, accumulation processes occurred in 22.14% (85 out of 384) of transects on the mainland coast. The shoreline shifted towards the sea within  $20.30 \pm 1.04$  m, with an average speed of  $0.57 \pm 0.03$  m/year (Figure 7). Erosion during this period accounted for 43.23% (166 out of 384) of transects, and the shoreline shifted towards the mainland at an average velocity of  $-0.70 \pm 0.02$  m/year; the NSM value was  $-24.84 \pm 0.74$  m. Stable shoreline was found in 34.64% (133 of 384) of transects. Significant coastal erosion extends at the northern pier of the Port of Klaipėda  $-56.9$  m in transect 413 (Figure 6). Accumulation processes in the accesses of Port of Klaipėda piers changed to intensive erosion, which in 2019 covered 700 m (28 transects) of the coast; the total NSM in them was  $-28.28$  m, the EPR value was  $-0.76 \pm 0.04$  m/year.

#### 4.2. Short-Term Shoreline Changes

Comparison of the shoreline changes in 1984–1990 and 1984–2019 showed that the area of eroded coast increased 2.7 times, from 1.50 km (60 transects) to 4.15 km (166 transects).

The effect of accumulation processes in 1984–2019 was recorded in 85 transects instead of 145 transects in 1984–1990. The accumulation rate decreased from  $4.33 \pm 0.11$  m/year to  $0.57 \pm 0.03$  m/year. The area of stable shores decreased from 3.325 km (133 transects) to 4.475 km (179 transects).

During the 1984–1990 period (Figure 8), the overall shoreline change was positive—the coast moved seawards on average  $23.95 \pm 0.76$  m. During this period, the predominant wind direction was W, WSW, and the average wind speed varied from 0 to 16 m/s.

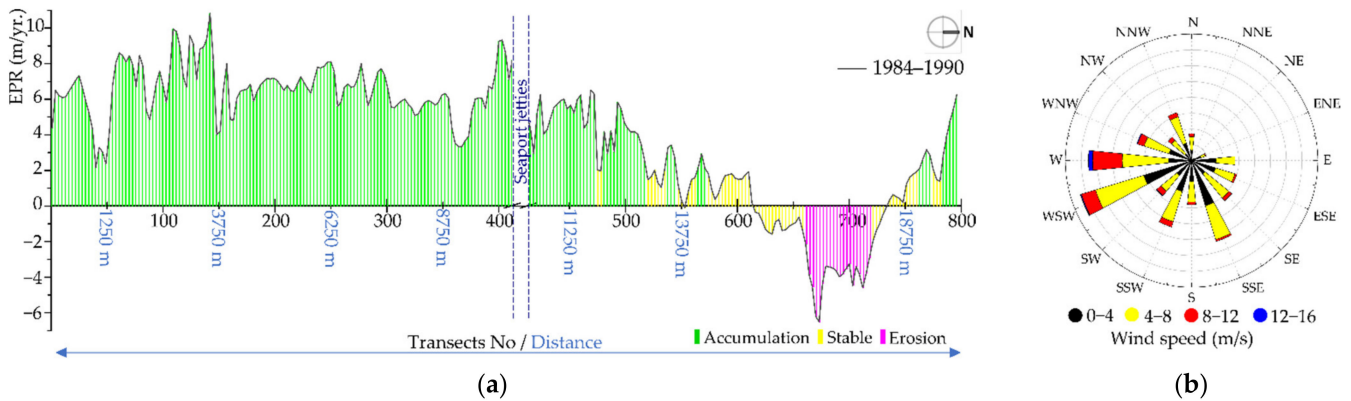


Figure 8. Graph showing the distribution of EPR (a) and wind rose (b) for 1984–1990.

Accumulation was detected in all transects of the Curonian Spit coast, where the shoreline moved seawards by 12.99–65.08 m with an average velocity of  $6.56 \pm 0.08$  m/year. On the mainland coast, the shoreline position changes were observed within the range of determination  $\pm 12.42$  m and can be considered as quasi-stable.

Coastal erosion was observed in a 1.5 km (60 transects) area to the north in the 6.2 km from the northern seaport jetty. The shoreline moved landward at an average velocity of  $-3.97 \pm 0.13$  m/year. The most significant negative change occurred in the 672nd transect and reached  $-41.58$  m. Accumulation occurred in 37.8% of transects on the mainland coast, and here the shoreline moved seawards, with an average velocity of  $4.33 \pm 0.11$  m/year.

In the 1990–1995 period (Figure 9), the coast has been intensively eroded, with the predominant 0–16 m/s W, WSW, SW wind direction. The shoreline moved landwards in 620 (77.9%) from 796 transects with an average of  $-22.85 \pm 0.46$  m. Significant changes in shoreline movement were observed in the immediate proximity of the seaport jetties. In the Curonian Spit coast, the maximum value of NSM was  $-100.85$  m and was detected in the 412rd transect, next to the southern Klaipėda seaport jetty (Figure 8). The most significant shoreline movement landwards was observed in a 250 m (402–412 transects) coastal area to the south from the southern seaport jetty. Here the shoreline moved toward land on average  $77.88 \pm 1.11$  m with an average velocity of (EPR)  $-15.58 \pm 0.22$  m/year.

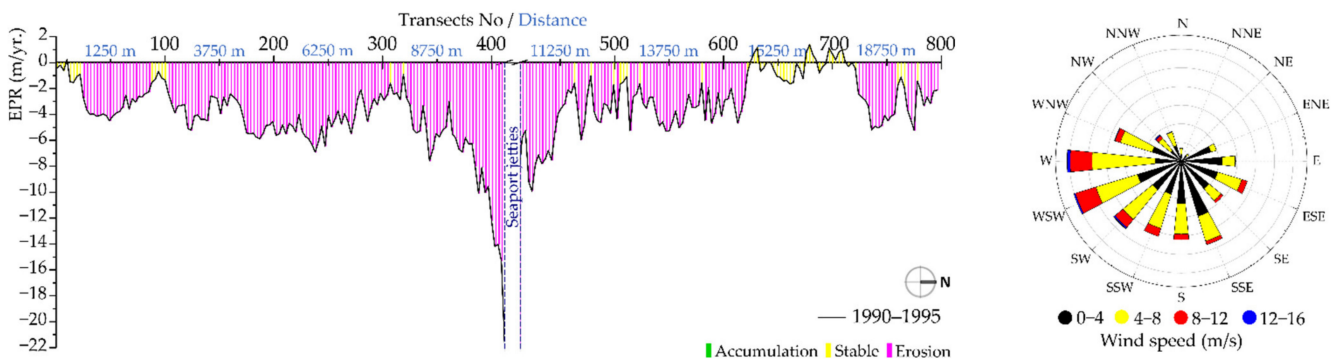


Figure 9. Graph showing the distribution of EPR (a) and wind rose (b) for 1990–1995.

65.9% of transects on the mainland coast can be described as erosive. The average change velocity reached  $-4.09 \pm 0.10$  m/year, and the shoreline moved landwards about  $-20.45 \pm 0.51$  m. The quasi-stable coast was observed in 131 transects (34.1%), and an average EPR value was  $0.44 \pm 0.08$  m/year. The most significant shoreline movement  $>30$  m was detected in the 419–443 transect. The maximum value was observed in the 424th transect and reached 49.61 m (EPR  $-9.92$  m/year).

The following ten years, 1995–2005, with the predominant SW, SSW, and WSW (0–16 m/s velocity) winds (Figure 10), had accumulative tendencies at the Curonian spit coast. The coast started recovery after the previous erosive period. Furthermore, hurricane Anatoly, which occurred in December 1999 [20], was not visible in the coastal evolution processes. It is evident that the quasi-stable part became erosive during the last five years at the mainland coast, and all other parts stayed accumulative.

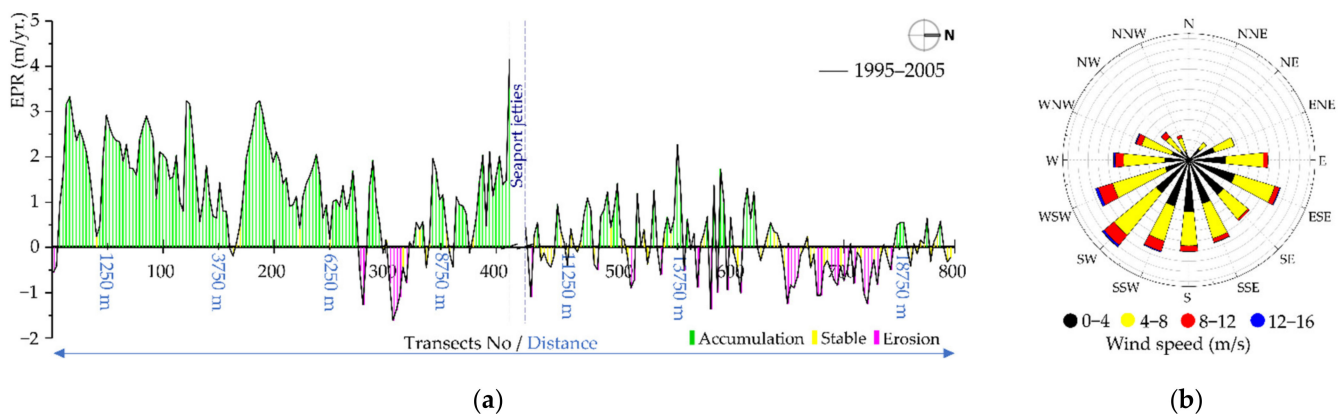


Figure 10. Graph showing the distribution of EPR (a) and wind rose (b) for 1995–2005.

The total change of the shoreline in the studied area in 1995–2005 was positive and amounted to  $6.72 \pm 0.39$  m with an EPR value of  $0.67 \pm 0.04$  m/yr. The Curonian Spit coast was characterized as accumulative. Here accumulation processes were observed in 320 transects from 412, and the accumulation rate was  $1.70 \pm 0.044$  m/yr. Erosion was observed in 27 transects (650 m). From 304 to 320 the transect EPR value was  $-1.00 \pm 0.03$  m/yr. From 277 to 282, the EPR value reached  $-0.86 \pm 0.10$  m/yr. The significant accumulation rate of 4.15 m/yr. (NSM 41.52) was noted in the immediate proximity of the jetties.

In the next five years, 2005–2010 (Figure 11), wind accumulation processes prevailed, with the WSW, SW, S, SE (0–12 m/s). In 61.1% of transects, the shoreline moved seawards with an averaged velocity of  $2.12 \pm 0.05$  m/yr., and NSM value reached  $10.62 \pm 0.25$  m.

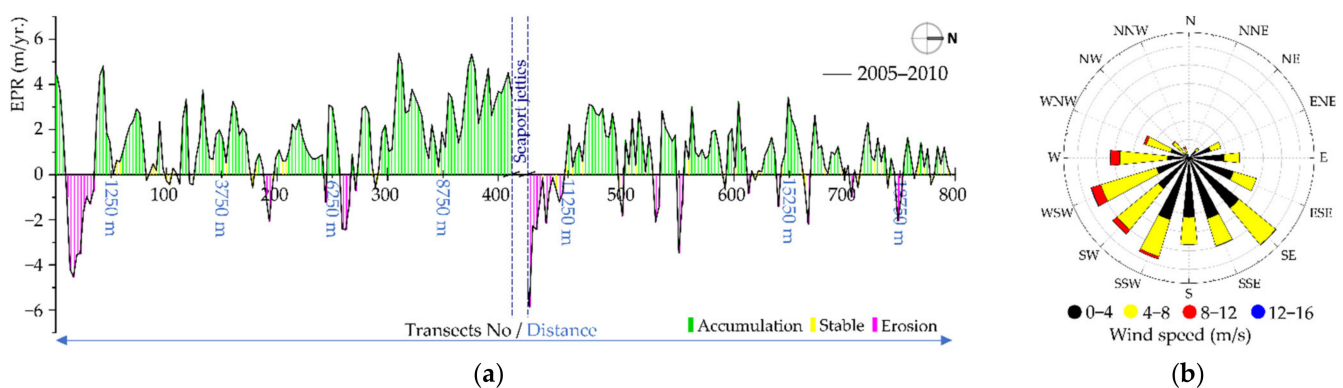


Figure 11. Graph showing the distribution of EPR (a) and wind rose (b) for 2005–2010.

Accumulation processes were more frequent on the Curonian Spit coast, which was observed in 67.7% of transects. The average velocity of shoreline movement seawards

was  $+2.42 \pm 0.07$  m/yr. During 2005–2010 the shoreline erosion on the Curonian Spit coast occurred only in 10.40% of transects that amounted to 1075 m out of 10.3 km. The significant erosive coastal stretch was found in the southern part of the Curonian Spit between 10 and 34 transects. In the 625 m section, the shoreline moved landwards, on average  $-12.82 \pm 0.29$  m (EPR  $-2.56 \pm 0.26$  m/yr). The maximum value of NSM was noted in the 26th transect and reached  $-26.69$  m.

On the mainland coast, accumulation was detected in 53.9% (270 out of 384) of transects, and the shoreline moved towards the sea by an average of  $8.62 \pm 0.28$  m. The average EPR value was  $1.73 \pm 0.06$  m/yr. Stable shoreline changes or changes in the shoreline determination uncertainty range within  $\pm 0.69$  m/yr were detected at 119 or 31% of transects. Coastal erosion was recorded in 15.1% of transects (58 transects), in which the shoreline moved landwards at an average speed of  $-2.01 \pm 0.19$  m/yr. The most significant adverse changes in the shoreline position were found between 413 and 446 transects. In this 850 m-long coast stretch, the shoreline shifted to the mainland on average by  $-9.64 \pm 0.28$  m (EPR was  $-1.93 \pm 0.06$  m/yr).

During the 2010–2015 period (Figure 12), with the predominant WSW, SW, S, SE (0–12 m/s) winds, accumulation processes were noticed in 94.9% of transects (391 out of 412 transects) on the coast of the Curonian Spit, in which the shoreline moved seawards at an average speed of  $3.40 \pm 0.09$  m/yr. In 50% of transects (206 out of 412 transects), the shoreline shifted from land to sea by an average of  $27.82 \pm 0.04$  m (NSM). The maximum value of NSM reached 49.67 m in the 318th transect.

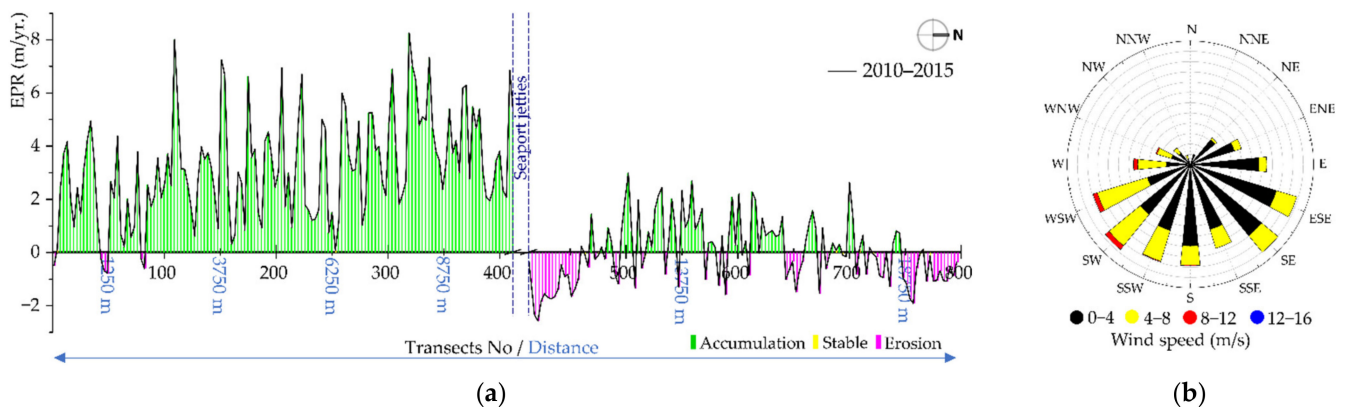


Figure 12. Graph showing the distribution of EPR (a) and wind rose (b) for 2010–2015.

On the mainland coast, erosive processes were observed during 2010–2015. Negative tendencies of shoreline displacement landwards were recorded in 47.4% of transects (182 out of 384), in which the shoreline generally shifted at an average speed of  $-0.51 \pm 0.07$  m/yr. The significant shoreline movement towards land was recorded in the 1175 m shoreline section north of the northern seaport jetty (between tr. 413 and 459). The average EPR value was  $-1.49 \pm 0.01$  m/yr, and the average NSM value was  $-8.63 \pm 0.07$  m; the maximum value of EPR was  $-2.57$  m/yr in 421 transects, and the maximum NSM value was  $-14.84$  m. The section of the shore from 746 to 796 transects stands out. This shore of 1275 m in 2010–2015 moved towards the sea in total  $-5.10 \pm 0.07$  m, and the erosion rate reached  $-0.88 \pm 0.01$  m/yr. The central part of the mainland coast was mainly formed by accumulation processes, which accounted for 41.9% of all transects (182 out of 284). The average accumulation rate in these transects was  $1.14 \pm 0.06$  m/yr, the value of NSM was  $6.80 \pm 0.34$  m. Stable shoreline fluctuations of about  $\pm 0.19$  m/yr were recorded in the 41st transect.

During the last analyzed period 2015–2019 (Figure 13), the predominant wind direction was WSW, SW, SWS, S, SSE (0–12 m/s velocity) and all of the coast was erosive. Over these 4 years, the shoreline moved seawards in 80.9% of transects (644 out of 796) with the average EPR value  $-4.24 \pm 0.12$  m/yr, and NSM —  $-15.91 \pm 0.46$  m.

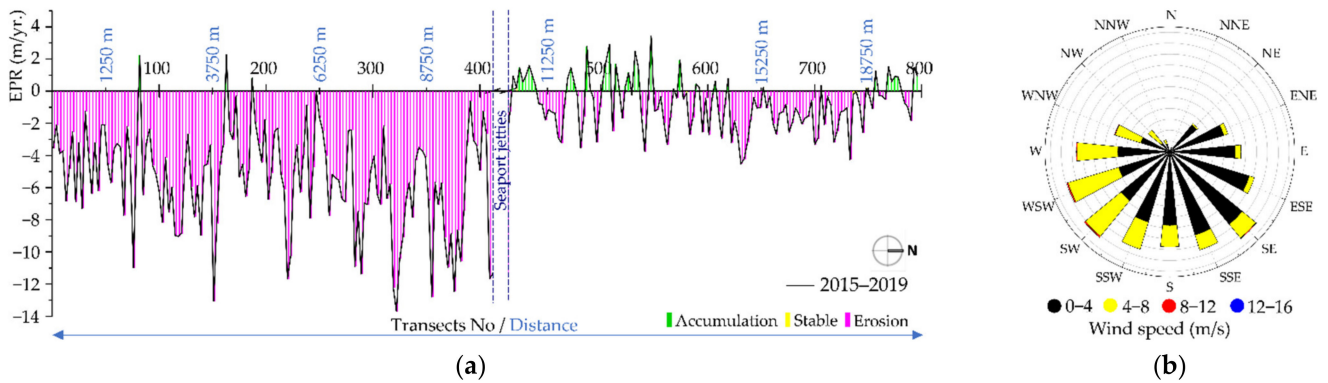


Figure 13. Graph showing the distribution of EPR (a) and wind rose (b) for 2015–2019.

On the Curonian Spit coast, erosion processes were detected at 97.3% of transects (401 out of 412) and were 3 times more intense than on the mainland. Here the EPR value reached  $-5.72 \pm 0.15$  m/yr., and the NSM respectively was  $-1.80 \pm 0.07$  m/yr.

The mainland coast moved seawards in 63.3% of transects (243 out of 384). In the southern part of the mainland coast, 105 transects (27.3%) were accumulative with an average velocity of  $1.30 \pm 0.08$  m/yr; here, the NSM value was  $4.86 \pm 0.29$  m.

In 2015, the Klaipėda seaport authorities started a nearshore nourishment project in front of the mainland coast (Figure 2). As a result, the additional sediments in the longshore sediment transport system led to milder coastal erosion on the mainland coast.

#### 4.3. Clusterization

K-Means cluster analysis was used to group the transects to identify stretches of shoreline with similar development tendencies. Net Shoreline Movement (NSM) values over the study period were grouped into five clusters (Figure 14). The NSM and SCE values and results of the cluster analysis distinguish different processes in different stretches of the Curonian Spit and the mainland coast and reflection of the influence of Klaipėda seaport piers on the morpho-lytodynamic processes of the coast.

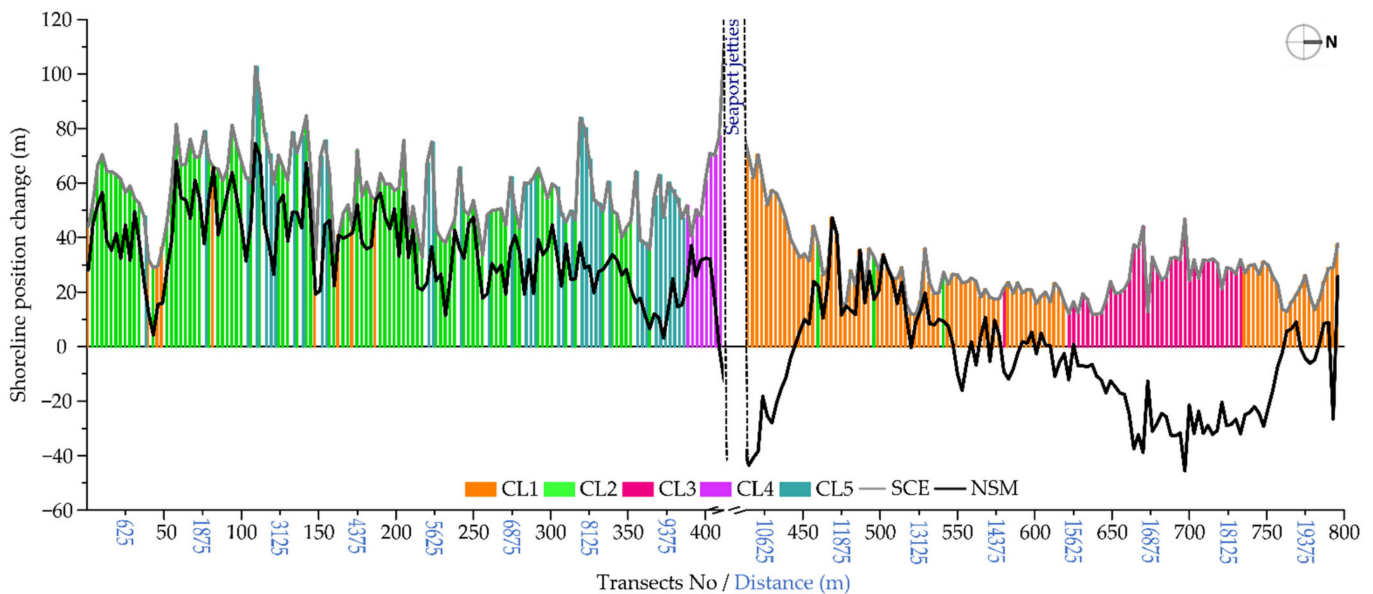


Figure 14. Graph showing the distribution of shoreline change envelope (SCE) (gray line) and net shoreline movement (NSM) (black line) along the study area for 1984–2019, and five clusters: cluster No. 1 (CL1), cluster No. 2 (CL2), cluster No. 3 (CL3), cluster No. 4 (CL4), cluster No. 5 (CL5).

The SCE corresponds closely with the NSM, implying that progressive and continuous change is more common than cyclical or reverse behavior in the spatial pattern of shoreline variability along the Curonian Spit. This stretch of coast connects Clusters No. 2 and No. 5, where the shoreline shifted towards the sea at an average of  $38.93 \pm 1.53$  m and  $27.66 \pm 2.17$  m, respectively (Table 1). Both clusters indicate accumulation processes on the coast. In cluster No. 2, the accumulation rate was  $1.10 \pm 0.04$  m/yr., the SCE range was 65.14 m. In cluster No. 5, the shoreline moved towards the sea at an average velocity of  $0.78 \pm 0.06$  m/yr. The SCE ranged between 38.01 m and 102.62 m (64.61 m). Moreover, on the coast of the Curonian Spit, Cluster No. 4 enters the southern port pier impact zone, which includes 27 transects (675 m long shoreline), where the shoreline may have different trends onshore dynamics at different times depending on hydrometeorological conditions. During the study period, the total change of the shoreline position in this cluster was positive and reached  $20.74 \pm 5.52$  m, and the accumulation speed was  $0.58 \pm 0.16$  m/yr. NSM values in this cluster ranged from  $-11.66$  to  $37.07$  m.

The SCE closely corresponds with NSM along the mainland coast, except for the 445 and 547 transect section. The section of Cluster No. 1 is alternating, mainly due to anthropogenic activity, such as beach nourishment.

The majority (67.2%) of the mainland coast transects belong to cluster No. 1 (No. 2—3.1%, No. 3—29.7%). Four coast sections can be distinguished in this area, where the shoreline has different movement tendencies in the transects in the 675 m long section of the coast (from 415 to 442 tr.) North of the northern port jetty, erosion processes took place during the study period. The average erosion rate (EPR) was  $-0.64 \pm 0.04$  m/year, and the NSM value was  $-24.59 \pm 1.31$  m. The NSM range covered values from  $-4.19$  m to  $-43.49$  m, with a mean SCE of  $56.74 \pm 0.96$  m. From 445 to 547 transects, the shoreline position changed at an average speed of  $0.47 \pm 0.01$  m/year. The total NSM in transects was  $16.67 \pm 0.36$  m. from  $-0.33$  m to  $47.25$  m. SCE from 11.8 m to  $47.25$  m. In 2014–2018, by order of the Klaipėda seaport Authority,  $237.78 \times 10^3$  m<sup>3</sup> of sand was dumped on the coast near the beaches of Melnragė-Giruliai (Figure 2).

Another group of transects from 519 to 619 in Cluster No. 1 showed slightly negative shoreline position changes, in which the shoreline moved towards the mainland during the study period by  $-0.05 \pm 0.01$  m/yr., the mean NSM value was  $-1.93 \pm 0.30$  m. SCE ranges from 15.78 m to 26.37 m, NSM from  $-16.07$  to  $10.73$  m. In the northern part of cluster No. 1, from 736 to 796 transects, changes in the shoreline influenced by erosive processes were recorded. Here the shoreline changed at an average velocity of  $-0.20 \pm 0.02$  m/yr. NSM was  $-7.15 \pm 0.72$  m (from  $-29.23$  to  $25.7$  m), SCE covered an overall change of  $23.83 \pm 0.32$  m and ranged from 12.82 m to 37.52 m.

Cluster No. 3 covers the central part of the mainland coast and indicates transects in which negative trends in shoreline dynamics have occurred during the study period. The shoreline of the 117 transects of this cluster moved towards the mainland at an average velocity of  $-0.64 \pm 0.05$  m/yr. The overall change in NSM was  $-22.70 \pm 1.74$  m.

This indicates the accretion processes in the Curonian Spit coast. The clusterization approach also suggests the accretion processes on the Curonian Spit coast with positive values of SCE and NSM (Table 3).

**Table 3.** Net Shoreline Movement (NSM) values and Shoreline Change Envelope (SCE) values per cluster.

Clusters No.	Transects No.	SCE (m)			NSM (m)		
		Mean	Min	Max	Mean	Min	Max
1	285	$29.34 \pm 1.38$	11.8	70.36	$4.07 \pm 2.07$	-43.49	65.62
2	255	$55.74 \pm 1.44$	27.29	92.43	$38.93 \pm 1.53$	4.3	69.97
3	117	$25.41 \pm 1.41$	11.92	46.76	$-22.70 \pm 1.74$	-45.53	0.7
4	27	$64.25 \pm 6.91$	40.51	108.85	$20.74 \pm 5.52$	-11.66	37.07
5	114	$62.68 \pm 2.18$	38.01	102.62	$27.66 \pm 2.17$	3.13	74.44

#### 4.4. Meteorological Data Analysis

Changes in the wind direction are determined as the primary driver for sediment transport and drive coastal erosion [1,16,43,44]. The long-term wind direction and velocity at the studied area were analysed to indicate such changes.

The time series of yearly mean wind direction at Klaipėda is presented in Figure 15, and demonstrates changes in the regime of wind direction in the 1960–2019 period and suggests that at least two regime shifts have occurred during this period. The regime shift timings are found using a cut-off length of 10 years and Hubert’s weight parameter of 1 [42]. This method detected that from 1960 till 1992, the wind direction on average was 216° (SW), then an average direction shifted to 188° (S), and the recent shift that occurred in 2011 was to 177° (S). The applied Rodionov regime shift method indicates that the average wind direction is shifting to the southern direction.

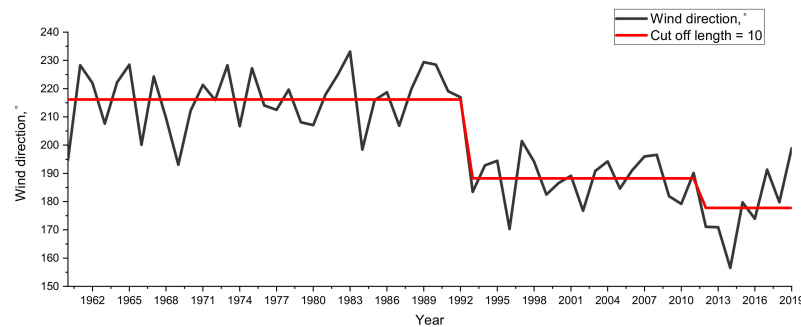


Figure 15. A shift in the annual average wind direction in Klaipėda in 1960–2019.

The first observed regime shift in the mean values of wind direction occurred in 1992 (Figure 15). At this point, we observed that the wind direction shifted to the west–south direction. This change in the regime coincides with the changes in the shoreline that occurred when erosion was observed both on the Curonian Spit and on the mainland coast. Another detected regime shift occurred in 2011 with the same shift to the southern direction. During this period on the mainland coast, erosion processes were observed, and accumulation prevailed on the Curonian Spit coast.

The frequency distribution (Figure 16) of the predominant wind direction at Klaipėda in the 1960–2019 period determines that the predominant wind, up to 1995, was 270° (W). The applied Rodionov shift detection method (Figure 15) confirms that in 1995 the predominant wind direction shifted to 209° (SSW).

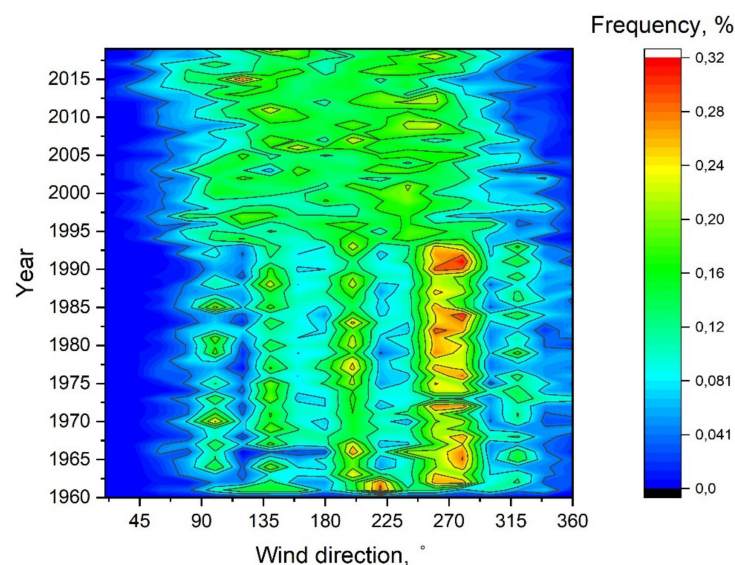


Figure 16. Frequency of occurrence wind directions at Klaipėda in 1960–2019.



## 5. Discussion

The Port of Klaipėda jetties location interrupts the natural longshore sediment transport path from the south to north at this point of the South-East Baltic Sea [6,23,45,46]. This should create favorable conditions for the two different processes: accumulation on the Curonian Spit south of the jetties and erosive—north of the jetties. Although the long-term analysis of shoreline changes in the whole study area indicates a total positive shoreline shift towards the sea, on the average velocity of  $0.43 \pm 0.03$  m/yr, over the 35 years, the shoreline had different trends in both geomorphological and temporal changes. From the long-term perspective, the 10 km long Curonian Spit coast to the south of the southern Klaipėda seaport jetties is attributed to the accumulating coastal stretch. The mainland coast encompassing the northern part of the study site is affected by erosive processes.

The jetties seaport systems on a straight sandy shore block the natural littoral drift [47,48], which determines the development of shoreline configurations. Typically, an up and down littoral drift is formed when hard breaking structures interrupt the predominant sediment transport direction. Due to the prevailing W and SW winds off the coast of Lithuania, sand transport is directed from south to north [49–52]. As a result, up-drift accretion occurs on the Curonian Spit coast on the south side of the jetties. Down-drift erosion occurs after losing its replenishment to maintain stability on the mainland coast (on the north side of the jetties).

The morphological changes of sandy beaches occur rapidly on a spatio-temporal scale as a response to natural (wind direction and speed, wave climate, sea-level fluctuations, etc.) processes [53]. Signs of climate change in the Baltic Sea can be more than just seawater level rise [54–56], increase in storminess [1], but also changes in the predominant wind and wave climate [43]. The climate change indicator in the wind regime is characterized as increasing in the wind velocity or intense wind events and changes in the predominant wind direction. This indicates changes in the cyclone patches over the Baltic Sea [57]. Changes in the wind direction and wave climate can alter longshore sediment transport magnitude and the dominant direction [58,59].

During this study, changes were observed in the predominant wind direction since 1992 (Figure 14), when the first regime shift occurred. The second shift in the wind direction regime was observed in 2012 (Figure 14). Significant changes in the predominant coastal evolution processes were observed after the wind direction shifts. Observed shifts of wind direction regime correspond with short-term changes of shoreline dynamics.

Shifts of wind direction regimes influenced intensified coastal erosion on both the Curonian Spit and the mainland coasts. In particular, the change in the wind direction regime influenced the short-term development of the Curonian Spit coast. In the periods of 1990–1995 and 2015–2019, the degree of erosion on this coast reached the respective levels of  $4.57 \pm 0.09$  and  $4.24 \pm 0.12$  m/year. The shoreline movement tendency of the 19th century was observed when the shoreline shifted towards the sea on both the Curonian Spit and the mainland coast [21]. This tendency reoccurred in the period of 2015–2019, on the usually accumulative Curonian Spit coast, which became erosive, while the average rate of erosion processes on the mainland coast decreased. In order to identify shoreline movement changes related to shifts in hydrometeorological conditions, a detailed investigation of wave climate (height, direction, period), sea-level fluctuations, and stormy events is required. Wave climate is driven by the wind climate [1,60] combined with the wind-driven coastal currents, and these are the major drivers for erosion and sedimentation, especially along the sandy sections of sandy beaches, dunes and soft moraine cliffs [2,61]. Future coastal process predictions are complicated as potential changes in the long-term mean and extreme wind speeds have a high uncertainty rate [1,62].

Moreover, significant changes in shoreline dynamics were observed in periods after the 2002 Klaipėda seaport reconstruction. Intensive erosion was observed on the mainland coast in the nearest proximity to the seaport jetties. Erosion after the reconstruction is acknowledged in other authors' [13,63] research. However, nowadays, as well as in the

past, the main factor for the coastal erosion processes was attributed to dredging works in the Klaipėda seaport and especially in port jetty area [22,64].

Dredging works are carried out to maintain proper water levels in fairways, waterways, and ports. Work related to the extraction of bottom sediments includes various areas of activity related to their extraction, transportation, storage, cleaning, and practical use. Dredging works disturb the natural integrity of bottom sediments (benthos) and directly and indirectly impact all marine environment elements [65,66]. Sediments excavated from the Baltic Sea coast are stored in designated areas at sea or on land. Such sites are usually located near port areas for economic motives [65]. Current environmental trends encourage the recycling or practical use of excavated sediments. One of the essential practical advantages is the beach nourishment with extracted sand if it meets the established physical and chemical properties. Artificial sand nourishment can be used as a coastal erosion mitigating measure by adding sediments directly to the coast or supplementing the natural longshore sediment transport budget.

In 2014–2018, by order of the Klaipėda seaport Authority,  $237.78 \times 10^3 \text{ m}^3$  of fine sand was dumped on the nearshore beaches of Melnragė-Giruliai at 4–6 m depth (Figure 4). The extracted sediments from the Klaipėda strait were used to restore the mainland sediment budget and replenish the coast. Beach sand nourishment is a widely known method to widen and restore the subaerial beach and decrease coastal erosion [67–69]. The nourishment material redistribution is driven by local hydrodynamic conditions (waves and currents). The predominant longshore current is directed from south to north along the Lithuanian coast [49,51]. Therefore, to mitigate the disrupted natural sediment transport by Klaipėda seaport jetties, the sediment dumping areas are located north of Klaipėda seaport jetties (Figure 4). The grain size distribution of the sand is dominated by grains with a size of 0.1–0.25 mm, representing 70–96% of grains with an Md between 0.14 mm and 0.22 mm, which corresponds precisely to the composition of the beach sand. Such sand composition detected on the mainland coast indicates that the nourishment material is transported in a predominant longshore direction and significantly influences cross-shore profile evolution.

Understanding the short- and long-term variability of the shoreline changes could help design shore nourishment in such a way that anthropogenic activity would be carried out in coherence with natural processes rather than in conflict [70,71]. Usually, shoreline change rates are best suited for the quasi-linear trend analysis. However, values of the shoreline variation are often non-linear and have different trend reversals. It is possible to single out the behaviors of certain groups that have the same or similar tendencies of change when using a joint shoreline change rates trend and cluster-based segmentation analysis.

According to K-means clustering of long-term changes in five different short-term periods in 796 transects, 369 transects covering clusters No. 2 and No. 5 are essentially distributed at the Curonian Spit and indicate accumulation processes. The positive dynamic characteristics of this coastal stretch are essentially in line with the multi-year shoreline changes in this coast type. Moreover, they reflect the main geomorphological and sedimentary conditions of the Curonian Spit.

The Klaipėda seaport impact zone was reflected in clusters No. 1 and No. 5. Still, cluster No. 1 identifies significant anthropogenic activities or impacts on the mainland coastal stretch due to shore replenishment. At the same time, on the mainland coast further from the direct port jetties impact area [20,28], Cluster No. 3 shows the presence of other factors with a more significant impact on the shoreline evolution. The trend in the SCE indicator also distinguishes the accumulative stretch of shore from 445 to 550 transects, which proves the impact of damping of the dredged sand from the Klaipėda strait.

## 6. Conclusions

Forecasting and continuous estimation of the intensity of the sandy South-Eastern Baltic Sea coast dynamics are essential to customizing coastal development management methods and techniques that affect the nature and economics of the coastal environment. The analysis of long- and short-term shoreline changes should provide the required knowl-

edge for reducing the extent of the anthropogenic intervention factors into the natural coastal system with long-lasting consequences.

This study aims to qualitatively and quantitatively identify the sandy South-Eastern Baltic Sea coast shoreline evolution tendencies. The reconstruction of Klaipėda jetties disrupted the settled equilibrium stage, interrupted the longshore sediment transport, and activated erosion processes. As a result, in the long-term (1984–2019) perspective, the northern part of the coast became abrasive, eroded coast length increased three times, from 1.5 to 4.2 km.

Assessment of short-term shoreline changes combined with K-means cluster analysis has helped identify the direct impact zone of the Port of Klaipėda. In this study, short-term shoreline changes correspond with shifts in wind direction and reflect the effect of the dredging works in the Klaipėda strait. The research helped identify the part of the mainland coast (transects from 445 to 550) that acquires other dynamic properties of the shore—accumulation. Although according to the hydrometeorological and litho-geomorphological characteristics and the impact of the port, erosion processes should prevail. It occurs due to coastal zone nourishment works. Therefore, this site needs continuous research because it is sensitive to anthropogenic and meteorological conditions. It also requires regular monitoring of the coast nourishment, as the development of coastal infrastructure, coastal use for recreational purposes, and planning of coastal protection measures depend on it.

**Author Contributions:** Conceptualization, V.K.; methodology, V.K., L.K.-R. and I.Š.; software, V.K.; validation, V.K., I.Š. and E.B.; formal analysis, V.K.; investigation, I.Š.; data curation, V.K., E.B. and I.Š.; writing—original draft preparation, V.K.; writing—review and editing, I.Š. and E.B.; visualization, V.K. and I.Š.; supervision, L.K.-R. All authors have read and agreed to the published version of the manuscript.

**Funding:** The APC was funded by Lithuanian science foundation project “Development of doctoral studies” Nr. 09.3.3-ESFA-V-711-01-0001. Kelpšaitė-Rimkienė was also supported by the Baltic Research Programme (EEA Financial Mechanisms 2014–2021) project “Solutions to current and future problems on natural and constructed shorelines, eastern Baltic Sea” (EMP480).

**Institutional Review Board Statement:** Not applicable.

**Informed Consent Statement:** Not applicable.

**Data Availability Statement:** The data presented in this study are available on request from the corresponding author.

**Acknowledgments:** We would like to thank the Klaipėda State Seaport Authority for supporting this research and providing data.

**Conflicts of Interest:** The authors declare no conflict of interest.

## References

1. Weisse, R.; Dailidienė, I.; Hünicke, B.; Kahma, K.; Madsen, K.; Omstedt, A.; Parnell, K.; Schöne, T.; Soomere, T.; Zhang, W.; et al. Sea Level Dynamics and Coastal Erosion in the Baltic Sea Region. *Earth Syst. Dyn. Discuss.* **2021**, *12*, 871–898. [[CrossRef](#)]
2. Zhang, W.; Schneider, R.; Kolb, J.; Teichmann, T.; Dudzinska-Nowak, J.; Harff, J.; Hanebuth, T.J.J. Land-sea interaction and morphogenesis of coastal foredunes—A modeling case study from the southern Baltic Sea coast. *Coast. Eng.* **2015**, *99*, 148–166. [[CrossRef](#)]
3. Montaña, J.; Coco, G.; Cagigal, L.; Mendez, F.; Rueda, A.; Bryan, K.R.; Harley, M.D. A Multiscale Approach to Shoreline Prediction. *Geophys. Res. Lett.* **2021**, *48*. [[CrossRef](#)]
4. Davidson, M.A.; Splinter, K.D.; Turner, I.L. A simple equilibrium model for predicting shoreline change. *Coast. Eng.* **2013**, *73*, 191–202. [[CrossRef](#)]
5. Phillips, B.T.; Brown, J.M.; Bidlot, J.R.; Plater, A.J. Role of Beach Morphology in Wave Overtopping Hazard Assessment. *J. Mar. Sci. Eng.* **2017**, *5*, 1. [[CrossRef](#)]
6. Viška, M.; Soomere, P.D.T. *Sediment Transport Patterns along the Eastern Coasts of the Baltic Sea*; Tallin University of Technology: Tallin, Estonia, 2014.
7. Soomere, T.; Viška, M.; Lapinskis, J.; Räämet, A. Linking wave loads with the intensity of erosion along the coasts of Latvia. *Est. J. Eng.* **2011**, *17*, 359–374. [[CrossRef](#)]

8. Bulleri, F.; Chapman, M.G. The introduction of coastal infrastructure as a driver of change in marine environments. *J. Appl. Ecol.* **2010**, *47*, 26–35. [CrossRef]
9. Schlacher, T.A.; Dugan, J.; Schoeman, D.S.; Lastra, M.; Jones, A.; Scapini, F.; McLachlan, A.; Defeo, O. Sandy beaches at the brink. *Divers. Distrib.* **2007**, *13*, 556–560. [CrossRef]
10. Hegde, A.V. Coastal erosion and mitigation methods-Global state of art. *Indian J. Geo-Mar. Sci.* **2010**, *39*, 521–530.
11. Rashidi, A.H.M.; Jamal, M.H.; Hassan, M.Z.; Sendek, S.S.M.; Sopia, S.L.M.; Hamid, M.R.A. Coastal Structures as Beach Erosion Control and Sea Level Rise Adaptation in Malaysia: A Review. *Water* **2021**, *13*, 1741. [CrossRef]
12. Bezerra, M.O.; Pinheiro, L.; Morais, J.O. Shoreline Change of the Mucuripe Harbour Zones (Fortaleza-Ceará, Northeast of Brazil) 1972–2003 on JSTOR. Available online: <https://www.jstor.org/stable/26481755> (accessed on 15 December 2021).
13. Bagdanavičiūtė, I.; Kelpšaitė-Rimkienė, L.; Galinienė, J.; Soomere, T. Index based multi-criteria approach to coastal risk assesment. *J. Coast. Conserv.* **2019**, *23*, 785–800. [CrossRef]
14. Bagdanavičiūtė, I.; Kelpšaitė, L.; Daunys, D. Assessment of shoreline changes along the Lithuanian Baltic Sea coast during the period 1947–2010. *Baltica* **2012**, *25*, 171–184. [CrossRef]
15. Burningham, H.; French, J. Understanding coastal change using shoreline trend analysis supported by cluster-based segmentation. *Geomorphology* **2017**, *282*, 131–149. [CrossRef]
16. Kelpšaitė, L.; Dailidienė, I. Influence of wind wave climate change on coastal processes in the eastern Baltic Sea. *J. Coast. Res.* **2011**, *27*, 220–224.
17. Baltranaitė, E.; Kelpšaitė-rimkienė, L.; Povilanskas, R.; Šakurova, I.; Kondrat, V. Measuring the impact of physical geographical factors on the use of coastal zones based on bayesian networks. *Sustainability* **2021**, *13*, 7173. [CrossRef]
18. Bagdanavičiūtė, I.; Umgiesser, G.; Vaičiūtė, D.; Bresciani, M.; Kozlov, I.; Zaiko, A. GIS-based multi-criteria site selection for zebra mussel cultivation: Addressing end-of-pipe remediation of a eutrophic coastal lagoon ecosystem. *Sci. Total Environ.* **2018**, *634*, 990–1003. [CrossRef]
19. Žilinskas, G.; Pupienis, D.; Jarmalavičius, D. Possibilities of regeneration of palanga coastal zone. *J. Environ. Eng. Landsc. Manag.* **2010**, *18*, 92–101. [CrossRef]
20. Jarmalavičius, D.; Žilinskas, G.; Pupienis, D. Impact of Klaipda port jetties reconstruction on adjacent sea coast dynamics. *J. Environ. Eng. Landsc. Manag.* **2012**, *20*, 240–247. [CrossRef]
21. Žaromskis, R.P. *Baltijos Jūros Uostai: Monografija*; Vilnius University: Vilnius, Lithuania, 2008; ISBN 9789955332510.
22. Žilinskas, G.; Janušaitė, R.; Jarmalavičius, D.; Pupienis, D. The impact of Klaipėda Port entrance channel dredging on the dynamics of coastal zone, Lithuania. *Oceanologia* **2020**, *62*, 489–500. [CrossRef]
23. Demereckas, K. *Klaipėdos Uostas = Port of Klaipėda*; Libra Mamelensis: Klaipėda, Lithuania, 2007.
24. History. Available online: <https://www.portofklaipeda.lt/history> (accessed on 14 November 2021).
25. Vareikis, V.; Bareiša, E. *Technika ir Gamta: Klaipėdos Uostas XIX a. Pabaigoje—XX a. Pirmojoje Pusėje = Technology and Nature: The Port of Klaipėda in the End of the 19th and the First Half of the 20th Century*; Klaipėdos Apskritis Archyvas: Klaipėda, Lithuania, 2014; ISBN 9789955188148.
26. Kelpšaitė-Rimkienė, L.; Soomere, T.; Bagdanavičiūtė, I.; Nestickeite, L.; Žalys, M. Measurements of Long Waves in Port of Klaipėda, Lithuania. *J. Coast. Res.* **2018**, *85*, 761–765. [CrossRef]
27. Ministry of Transport and Communications of the Republic of Lithuania. *The Master Plan of the Port of Klaipėda (Land, Internal Water Area, External Raid, and Related Infrastructure) N. 15088*; Ministry of Transport and Communications of the Republic of Lithuania: Vilnius, Lithuania, 2019.
28. Pupienis, D.; Jonuškaitė, S.; Jarmalavičius, D.; Žilinskas, G. Klaipėda port jetties impact on the Baltic Sea shoreline dynamics, Lithuania. *J. Coast. Res.* **2013**, *165*, 2167–2172. [CrossRef]
29. Bitinas, A.; Žaromskis, R.; Gulbinskas, S.; Damušyte, A.; Žilinskas, G.; Jarmalavičius, D. The results of integrated investigations of the Lithuanian coast of the Baltic Sea: Geology, geomorphology, dynamics and human impact. *Geol. Q.* **2005**, *49*, 355–362.
30. Bitinas, A.; Aleksa, P.; Damušytė, A.; Gulbinskas, S.; Jarmalavičius, D.; Kuzavinas, M.; Minkevičius, V.; Pupienis, D.; Trimonis, E.; Šečkus, R.; et al. *Baltijos Jūros Lietuvos Krantų Geologinis Atlasas*; Geological Survey of Lithuania: Vilnius, Lithuania, 2004.
31. Thieler, E.R.; Himmelstoss, E.A.; Zichichi, J.L.; Ergul, A. *The Digital Shoreline Analysis System (DSAS) Version 4.0—An ArcGIS Extension for Calculating Shoreline Change*; Open-File Report; U.S. Geological Survey: Reston, VA, USA, 2009. [CrossRef]
32. Himmelstoss, E.A.; Henderson, R.E.; Kratzmann, M.G.; Farris, A.S. *Digital Shoreline Analysis System (DSAS) Version 5.0 User Guide*; Open-File Report 2018–1179; U.S. Geological Survey: Reston, VA, USA, 2018; Volume 126.
33. Oyedotun, T.D.T. Shoreline Geometry: DSAS as a Tool for Historical Trend Analysis. *Geomorphol. Tech.* **2014**, *2*, 1–12.
34. Byrnes, M.R.; Anders, F.J. Accuracy of Shoreline Change Rates as Determined From Maps and Aerial Photographs. *Shore Beach Obs.* **2016**, *58*, 30.
35. Dolan, R.; Fenster, M.S.; Holme, S.J. Temporal analysis of shoreline recession and accretion. *J. Coast. Res.* **1991**, *7*, 723–744.
36. Fletcher, C.; Rooney, J.; Barbee, M.; Lim, S.; Beach, W.P.; Fletchert, C.; Rooney, J.; Barbeef, M.; Limf, S.; Richmond, B. Mapping Shoreline Change Using Digital Orthophotogrammetry on Maui, Hawaii Stable URL Linked References are Available on JSTOR for This Article: Mapping Shoreline Change Using Digital Orthophotogrammetry on Maui. *J. Coast. Res.* **2003**, *18*, 106–124.
37. Crowell, M.; Leatherman, S.P.; Buckley, M.K. Shoreline Change Rate Analysis: Long Term Versus Short Term Data. *Shore Beach* **1993**, *61*, 13–20.

38. Laccetti, G.; Lapegna, M.; Mele, V.; Romano, D.; Szustak, L. Performance enhancement of a dynamic K-means algorithm through a parallel adaptive strategy on multicore CPUs. *J. Parallel Distrib. Comput.* **2020**, *145*, 34–41. [[CrossRef](#)]
39. Kanungo, T.; Mount, D.M.; Netanyahu, N.S.; Piatko, C.; Silverman, R.; Wu, A.Y. An Efficient *k*-Means Clustering Algorithm: Analysis and Implementation 1 Introduction. In Proceedings of the 16th Annual Symposium on Computational Geometry, New York, NY, USA, 12–14 June 2000; pp. 1–21.
40. Kelpšaitė-Rimkienė, L.; Parnell, K.E.; Žaromskis, R.; Kondrat, V. Cross-shore profile evolution after an extreme erosion event—Palanga, Lithuania. *J. Mar. Sci. Eng.* **2021**, *9*, 38. [[CrossRef](#)]
41. Likas, A.; Vlassis, N.; Verbeek, J. The global k-means clustering algorithm. *Pattern Recognit.* **2003**, *36*, 451–461. [[CrossRef](#)]
42. Rodionov, S.N. A sequential algorithm for testing climate regime shifts. *Geophys. Res. Lett.* **2004**, *31*, 2–5. [[CrossRef](#)]
43. Soomere, T.; Pindsoo, K. Spatial variability in the trends in extreme storm surges and weekly-scale high water levels in the eastern Baltic Sea. *Cont. Shelf Res.* **2016**, *115*, 53–64. [[CrossRef](#)]
44. Bagdanavičiute, I.; Kelpšaitė, L.; Soomere, T. Multi-criteria evaluation approach to coastal vulnerability index development in micro-tidal low-lying areas. *Ocean Coast. Manag.* **2015**, *104*, 124–135. [[CrossRef](#)]
45. Gudelis, V. *Lietuvos Jūris ir Pajūris = The Lithuanian offshore and Coast of the Baltic Sea: Monograph*; Science and Arts of Lithuania: Vilnius, Lithuania, 1998; ISSN 132-4044.
46. Dean, R.G.; Dalrymple, R.A. *Coastal Processes with Engineering Applications*; Cambridge University Press: Cambridge, UK, 2001; ISBN 9780521495356.
47. De Boer, W.; Mao, Y.; Hagenaaars, G.; de Vries, S.; Slinger, J.; Vellinga, T. Mapping the sandy beach evolution around seaports at the scale of the African continent. *J. Mar. Sci. Eng.* **2019**, *7*, 151. [[CrossRef](#)]
48. Bruun, P. The Development of Drowned Erosion Author (s): Per Bruun Stable URL. The Development of Drowned Erosion. *J. Coast. Res.* **1995**, *11*, 1242–1257.
49. Viška, M.; Soomere, T. Simulated and observed reversals of wave-driven alongshore sediment transport at the eastern Baltic sea coast. *Baltica* **2013**, *26*, 145–156. [[CrossRef](#)]
50. Krek, A.; Stont, Z.; Ulyanova, M. Alongshore bed load transport in the southeastern part of the Baltic Sea under changing hydrometeorological conditions: Recent decadal data. *Reg. Stud. Mar. Sci.* **2016**, *7*, 81–87. [[CrossRef](#)]
51. Pupienis, D.; Buynevich, I.; Ryabchuk, D.; Jarmalavičius, D.; Žilinskas, G.; Fedorovič, J.; Kovaleva, O.; Sergeev, A.; Cichoń-Pupienis, A. Spatial patterns in heavy-mineral concentrations along the Curonian Spit coast, southeastern Baltic Sea. *Estuar. Coast. Shelf Sci.* **2017**, *195*, 41–50. [[CrossRef](#)]
52. Žilinskas, G.; Jarmalavičius, D.; Pupienis, D. The influence of natural and anthropogenic factors on grain size distribution along the southeastern Baltic spits. *Geol. Q.* **2018**, *62*, 375–384. [[CrossRef](#)]
53. Benkhattab, F.Z.; Hakkou, M.; Bagdanavičiūtė, I.; El Mrini, A.; Zagaoui, H.; Rhinane, H.; Maanan, M. Spatial-temporal analysis of the shoreline change rate using automatic computation and geospatial tools along the Tetouan coast in Morocco. *Nat. Hazards* **2020**, *104*, 519–536. [[CrossRef](#)]
54. Chechko, V.A.; Chubarenko, B.V.; Boldyrev, V.L.; Bobykina, V.P.; Kurchenko, V.Y.; Domnin, D.A. Dynamics of the marine coastal zone of the sea near the entrance moles of the Kaliningrad Seaway Channel. *Water Resour.* **2008**, *35*, 652–661. [[CrossRef](#)]
55. Soomere, T.; Viška, M. Simulated wave-driven sediment transport along the eastern coast of the Baltic Sea. *J. Mar. Syst.* **2014**, *129*, 96–105. [[CrossRef](#)]
56. Dailidienė, I.; Davulienė, L.; Tilickis, B.; Stankevičius, A.; Myrberg, K. Sea level variability at the Lithuanian coast of the Baltic Sea. *Boreal Environ. Res.* **2006**, *11*, 109–121.
57. Lehmann, A.; Höflich, K.; Post, P.; Myrberg, K. Pathways of deep cyclones associated with large volume changes (LVCs) and major Baltic inflows (MBIs). *J. Mar. Syst.* **2017**, *167*, 11–18. [[CrossRef](#)]
58. Dada, O.A.; Li, G.; Qiao, L.; Ma, Y.; Ding, D.; Xu, J.; Li, P.; Yang, J. Response of waves and coastline evolution to climate variability off the Niger Delta coast during the past 110 years. *J. Mar. Syst.* **2016**, *160*, 64–80. [[CrossRef](#)]
59. Chowdhury, P.; Behera, M.R. Effect of long-term wave climate variability on longshore sediment transport along regional coastlines. *Prog. Oceanogr.* **2017**, *156*, 145–153. [[CrossRef](#)]
60. Meier, H.E.M.; Kniebusch, M.; Dieterich, C.; Gröger, M.; Zorita, E.; Elmgren, R.; Myrberg, K.; Ahola, M.; Bartosova, A.; Bonsdorff, E.; et al. Climate Change in the Baltic Sea Region: A Summary. *Earth Syst. Dyn. Discuss.* 2021; in review. [[CrossRef](#)]
61. Harff, J.; Furmańczyk, K.; von Storch, H. *Coastline Changes of the Baltic Sea from South to East*; Springer: Berlin/Heidelberg, Germany, 2017; Volume 19, p. 386.
62. Räisänen, J. Future Climate Change in the Baltic Sea Region and Environmental Impacts. *Oxf. Res. Encycl. Clim. Sci.* **2017**, *1*, 1–39.
63. Jarmalavičius, D.; Pupienis, D.; Žilinskas, G.; Janušaitė, R.; Karaliūnas, V. Beach-foredune sediment budget response to sea level fluctuation. Curonian Spit, Lithuania. *Water* **2020**, *12*, 583. [[CrossRef](#)]
64. Žilinskas, G. Kranto Linijos Dinamikos Ypatumai Klaipėdos Uosto Poveikio Zonoje. *Geogr. Metraštis* **1998**, *31*, 99–109.
65. Staniszevska, M.; Boniecka, H. Managing dredged material in the coastal zone of the Baltic Sea. *Environ. Monit. Assess.* **2017**, *189*, 46. [[CrossRef](#)]
66. Rangel-Buitrago, N.; de Jonge, V.N.; Neal, W. How to make Integrated Coastal Erosion Management a reality. *Ocean Coast. Manag.* **2018**, *156*, 290–299. [[CrossRef](#)]
67. Ludka, B.C.; Guza, R.T.; O'Reilly, W.C. Nourishment evolution and impacts at four southern California beaches: A sand volume analysis. *Coast. Eng.* **2018**, *136*, 96–105. [[CrossRef](#)]

68. De Schipper, M.A.; Ludka, B.C.; Raubenheimer, B.; Luijendijk, A.P.; Schlacher, T.A. Beach nourishment has complex implications for the future of sandy shores. *Nat. Rev. Earth Environ.* **2021**, *2*, 70–84. [[CrossRef](#)]
69. Guillén, J.; Hoekstra, P. Sediment distribution in the nearshore zone: Grain size evolution in response to shoreface nourishment (Island of Terschelling, The Netherlands). *Estuar. Coast. Shelf Sci.* **1997**, *45*, 639–652. [[CrossRef](#)]
70. Hamm, L.; Capobianco, M.; Dette, H.H.; Lechuga, A.; Spanhoff, R.; Stive, M.J.F. A summary of European experience with shore nourishment. *Coast. Eng.* **2002**, *47*, 237–264. [[CrossRef](#)]
71. Pinto, C.A.; Silveira, T.M.; Teixeira, S.B. Beach nourishment practice in mainland Portugal (1950–2017): Overview and retrospective. *Ocean Coast. Manag.* **2020**, *192*, 105211. [[CrossRef](#)]